Atomic-number dependence of the secondary-electron cascade from solids

J. C. Greenwood, M. Prutton, and R. H. Roberts*
Department of Physics, University of York, Heslington, York YO1 5DD, England
(Received 18 October 1993)

The parameters A and m in the power-law expression for the kinetic-energy dependence of the secondary-electron cascade of solid elements has been measured as a function of the atomic number of the sample. A pattern has been observed in the values of both A and m which is related to the variations in the Periodic Table. m is found to fall between 0.5 and 1.5 as predicted by theory. Also, it has been established that the coefficient A is correlated with the exponent m. The measured values of m are expected to be related to the exponent of another power law of the kinetic energy which is found to describe the energy dependence of the electron attenuation length for energies above about 400 eV. This expectation is checked against several existing models or empirical expressions for the attenuation length. Moderate agreement is found between m and $(2-q)$ where q is the exponent of the energy dependence of the attenuation length described by Tokutaka *et al.* and the agreement is poorer with values of q derived from various theoretical treatments of the energy dependence of the inelastic mean free path. m is found to be correlated to the free-electron energy E_p and A to the density of valence electrons in the solid.

I. INTRODUCTION

In a series of papers beginning in 1977 Sickafus and co-worker[1-3] demonstrated that a reasonable theoretical description of the background function describing the energy dependence of the secondary-electron cascade from elements is given by

$$B(E)=AE^{-m}, \tag{1}$$

where $B(E)$ is the number distribution of electrons emitted with kinetic energy E from a solid. A and m are properties of the solid and A depends also upon the kinetic energy E_0 of the exciting beam. The theoretical justification of this form of the cascade was provided by examining the Boltzmann diffusion equation for spherically symmetric electron-electron scattering from a planar surface with a normally incident primary beam and extending the analysis from the conventional upper limit of 50 eV for the true secondary-electron region of the emission spectrum to about $0.5E_0$. This treatment was based upon earlier attempts to describe the shape of the secondary electron cascade due to Wolff[4] and improvements by others.[5-8] The theoretical treatment predicted that m would be independent of atomic number Z and with a value of unity. Sickafus reported experimental tests of Eq. (1) for Ni(110) and Cu(100) surfaces using a retarding field electron spectrometer. The cascade could indeed be linearized by plotting $\ln[B(E)]$ versus $\ln(E)$, as expected if Eq. (1) describes the experimental results. Further, this linearization was observed to occur in sections of the emission spectrum between the Auger peaks—the power m increasing below each family of Auger peaks and their associated losses. Sickafus worked with E_0 below 3 keV and showed that the parameter A in (1) varied approximately as $E_0^{-0.8}$ for the Ni(110) surface.

Further work by Strausser, Franklin, and Courtney[9] extended the applicability of cascade linearization via Eq. (1) to more complex materials and to the analysis of surface chemical composition after subtraction of this power law background shape from the emission spectrum. Peacock and co-workers[10,11] examined the effects on the constants in Eq. (1) of moving away from normal incidence and of using much higher primary energies. This work showed that, for InP(110), the exponent m was approximately independent of the angle of incidence in the range 0°–85° and that for a number of metallic and semiconducting elements the cascade shape was described accurately by Eq. (1) up to kinetic energies of 2 keV for primary energies in the range 15–22 keV. This higher primary beam energy is particularly important for studies of the emission cascade because the low-energy tail of the energetic rediffused primary electrons generated by a 20-keV beam is so weak below emission energies of 2 keV that the spectral shape is dominated by the cascade and any superimposed Auger features.

Matthew *et al.*[12] extended the theory proposed by Sickafus to include both generation of fast secondaries by electron Compton scattering and various approximations to the processes dominating the escape of the electrons to the vacuum and the spectrometer. The power-law cascade shape was retained in their results and, additionally, it was shown that, in the limit of vanishingly weak elastic scattering and an inelastic mean free path having an $E^{0.5}$ dependence, the value of m should be 0.5. In the limit of strong elastic scattering (the diffusion limit) the value of m should be 1.5. It was suggested that values of m found in elements should lie between these two values and results for eight different materials were presented, which confirmed this.

In order to produce standard reference spectra under defined conditions for Auger spectroscopy, it is extremely helpful to have some data that is representative of the properties of a sample and not the properties of the sample modified by the measuring system (the spectrometer has a transmission function, which distorts the true spec-

trum by multiplication and a transfer function, which broadens spectral features by convolution). Further, the shape of the background contains information about the physics of the electron-solid interaction, which can complement the information derived from spectral features such as peaks and absorption edges. This information may lead, for example, to a more detailed understanding of the subsurface chemistry and may be obtained without damaging the sample by depth profiling. Also, a known form of the background provides a physical basis for the means of subtracting a background function from beneath a peak in order to represent more accurately its shape and area for subsequent analysis.

This paper describes the results of measurements of the background shape for 32 elements and an examination of the atomic number dependence of the parameters A and m. These results are compared with the energy dependence of the attenuation lengths of electrons generated within the solid.

II. THEORY

By using Wolff's description of the electron transport process Sickafus[1] was able to show that the form of the cascade is given by

$$B(E)=a\sigma_0^{-1}(E)E^{-x}\ , \tag{2}$$

which leads, in turn, for a Bethe form of the total inelastic scattering cross section $\sigma_0(E)$, to the approximate expression

$$B(E)=DE_0^nE^{-m} \tag{3}$$

for a beam energy of E_0. In (3) D is a constant dependent upon Z and independent of energy, and DE_0^n is the parameter A in (1). This treatment leads to the values $x=2$, $m=1$, and $n=2$, which are independent of Z. As the inelastic mean free path (imfp), $\lambda(E)$, is inversely related to the total cross section $\sigma_0(E)$ and the number density of atoms or molecules N, Eq. (2) can be rewritten as

$$B(E)=aN\lambda(E)E^{-x}\ , \tag{4}$$

suggesting that the shape of the cascade and the energy dependence of the imfp should be related functions. The values of x, m, and n include the effects of the elastic scattering of electrons in the solid in the sense that a diffusion approach has been adopted to the escape of electrons into the vacuum. However, this is a simplification of the escape process in that it is a spherically symmetric scattering description for low-energy electrons (below 100 eV).

There has been a considerable amount of work reported on the calculation of $\lambda(E)$ (see, for example, the recent papers by Tanuma, Powell, and Penn,[13–16] and the references quoted therein). A formula, known as TPP-2, has been derived by them using imfp's calculated from experimental optical data and the Lindhard dielectric function. TPP-2 has been carefully compared with other, more pragmatically based, expressions for $\lambda(E)$.[13] In particular, a theoretical expression for the imfp has been suggested by Szajman *et al.*,[17] which is given by

$$\lambda(E)=SE^{3/4}(M/\rho N_v)^{1/2}\ , \tag{5}$$

where N_v is the number of valence electrons per atom, M the atomic weight and ρ the density. S is a constant.

On the other hand, there has been a large body of experimental work using x-ray-photoemission and Auger-peak-height measurements as a function of varying overlayer thicknesses in order to estimate the attenuation of electrons as they escape from the solid (see, for example, Briggs and Seah[18]). The characteristic attenuation length λ_{AL} derived from such experiments has been expressed, for the elements, as

$$\lambda_{AL}=538E^{-2}+0.41(aE)^{1/2}\ \text{monolayers} \tag{6}$$

by Seah and Dench[19] and

$$\lambda_{AL}=PE^q \tag{7}$$

by Wagner, Davis, and Riggs,[20] where a is the atomic size and P is a constant. Also, an expression developed from a reexamination of the data used by Seah and Dench supplemented by new experimental data and including effects due to the attenuation of the primary electron beam have been suggested by Tokutaka, Nishimori, and Hayashi.[21] For kinetic energies above about 400 eV all these expressions are approximately of the form in Eq. (7). Above 400 eV the exponent q is 0.5 for the attenuation length in expression (6) because the first term on the right-hand side of this equation becomes negligible compared to the second. From Eq. (5) the exponent q of the imfp is 0.75. Therefore, the characteristic lengths for inelastic scattering are independent of the atomic number of the solid in these two cases. However, the other expressions for the imfp's from Tanuma, Powell, and Penn and attenuation lengths from Tokutaka, Nishimori, and Hayashi require the exponent to be a function of Z. The various possibilities are compared in Fig. 1.

In order to compare the measured attenuation lengths with the theoretically derived imfp's, it is necessary to take some account of the effects of elastic scattering on the escape path length for electrons leaving the solid. Based upon theoretical work by Jablonski,[22] Seah[23] has proposed that the values of $\lambda(E)$ should be corrected to obtain an estimate of the attenuation length using

$$\lambda_{AL}=\lambda(E)\{1-0.028Z^{1/2}\}\{0.501+0.068\ln(E)\}\ . \tag{8}$$

This expression was obtained by fitting the values tabulated by Jablonski with functions of Z and E. The calculated values included the effects of single elastic events on the escape of Auger electrons from the solid but took no account either of multiple elastic scattering or the attenuation of the ingoing primary beam. It should be noted that application of this expression merely reduces the exponent describing the energy dependence of λ_{AL} but does not change the range of the exponent as a function of Z. Expression (8) has been used to modify TPP-2 and (5) in order to plot $\lambda_{AL}(Z)$ in Fig. 1. With this correction, Eq. (5) is modified to have an exponent of 0.82 independent of Z.

If an expression of the form (7) does describe the energy dependence of the imfp, then the transport equation

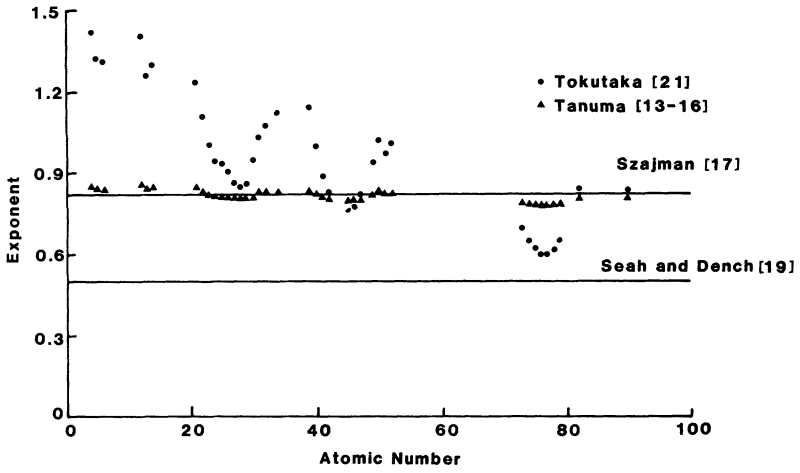

FIG. 1. Plot of various expressions for the exponent q of the energy dependence of the inelastic mean free paths and the attenuation lengths of the elements plotted as a function of the atomic number Z. The inelastic mean free paths have been modified to make a correction allowing approximately for the effects of elastic scattering on the escaping electrons (see text).

approach suggested by Matthew *et al.*[12] leads to the suggestion that the exponent m in Eq. (1) have a value between 0.5 and 1.5 and should have the value $(1-q)$ in the absence of elastic scattering effects. The case of strong elastic scattering together with an energy dependent imfp was not solved analytically but increasing the strength of elastic scattering is expected to increase m and the greater the energy dependence of the imfp the smaller is the expected value of m.

It is clear from the data sketched in Fig. 1 that the energy dependence of the λ_{AL}'s are very different from each other—some showing an atomic number dependence and some not. Variations across the rows of the Periodic Table are more pronounced in the Tokutaka, Nishimori, and Hayashi than in the modified form of the Tanuma, Powell, and Penn estimates of this parameter.

III. EXPERIMENT

A. Spectrometer characterization

The spectrometer used in this work is part of a multispectral Auger microscope constructed in the authors' laboratory. The instrument is described elsewhere.[24] The energy analyzer in this instrument is a 180° concentric hemispherical type (CHA) equipped with a four-element transfer lens and a position sensitive detector. For the spectroscopy reported here the spectrometer was operated as a single-channel device by adding all 15 output channels together. The energy resolution in this arrangement was approximately constant for kinetic energies between 100 and 2500 eV and was about 10 eV for a pass energy of 100 eV (the kinetic energy of the electrons as they traverse the space between the hemispheres). This resolution was chosen to give a large signal from the sample, which was illuminated with a 20-keV electron beam focused into a 200-nm-diam spot containing about 8 nA of current. It was adequate for a study of the background shape, which changes very slowly with energy and also the Auger peaks were still clearly resolved. During the acquisition of spectra, the beam was scanned over a square region about 80 μm on a side. This scanned area ensured that both the surface roughness and crystallite size of the samples were on a scale which was small compared to the area measured, so minimizing the effects of these two properties.

Any spectrometer modifies the true energy distribution of emitted electrons in the slowly varying background in two ways. The first is due to the spectrometer not passing electrons with different kinetic energies with the same efficiency. This leads to a transmission function characterizing the instrument, which generally has the form of decreasing efficiency with increasing kinetic energy. The topic has been carefully treated by Seah and is reviewed in Briggs and Seah.[18] The second arises from internal scattering of electrons within the spectrometer. Electrons entering the spectrometer with energies above the range that will be passed to the detectors can strike metallic components and generate secondary electrons. Some of these secondaries travel in appropriate directions with suitable kinetic energies to reach the detector and contribute to the measured spectrum. Thus internal scattering is an addition to the true electron spectrum as opposed to the transmission function, which usually causes a reduction in the height of the true spectrum. The relatively large internal scattering effects in CHA's have only recently been quantified and are described in papers by Seah and Smith,[25] Seah,[26] and Greenwood *et al.*[27]

The CHA used for the work described here was characterized in a series of experiments in which the pass energy of the hemispheres was varied and the internal scattering determined using Auger spectra from eight different elemental samples. The method has been described in detail by Seah and Smith[25,26] and the transmission function and internal scattering function for this spectrometer has been reported by Greenwood *et al.*[27] This pair of functions was then used to correct the measured spectra of pure Be and B samples, which are useful because of the large energy span of featureless spectrum from each of these materials. The values of A and m for these samples were then estimated using the corrected spectra from measurements with three different pass energies (50, 100, and 200 eV) around the hemispheres. The values of A and m were the same for the three pass energies within the experimental errors, which were deter-

mined by the signal to noise ratios in the raw data. Further, the same instrumental function was applied to all 32 elements whose spectra were collected and, in every case, the corrected shapes of the emission spectra were a good fit to Eq. (1). Therefore it was concluded that instrumental effects had been removed successfully from the data. Full details of the methods used for this careful characterization are given by Greenwood *et al.*[27] The spectrum from any material can be used for this characterization provided that it has a large energy range free of Auger peaks. Carbon is used in the present work because it satisfies this criterion and is easy to prepare with a surface free of common contaminants such as oxygen, chlorine and sulphur.

In order to achieve reproducibility in both the instrument function and the measured spectra, a number of procedures were adopted. (i) The sample holder was degaussed so that the magnetic fields in the regions between the electron gun and the sample and also the sample and the detector of the spectrometer were less than 1 μT everywhere. (ii) Insulating surfaces were arranged so that there were no line of sight to them from the point of impact of the primary beam. These two precautions avoided movements of the effective emission source and trajectory modifications due to magnetic fields and electrostatic charging in the vicinity of the sample. (iii) The specimen manipulator was used to place the sample in the center of the field of view of the spectrometer. Preliminary instrument calibration had ensured that the axis of the electron gun and its electron-optical column intersected the axis of the spectrometer transfer lens and that the sample could be manipulated to this intersection. The net effect of these three precautions was that the center of the area on the sample acting as a source of electrons leading to the measured spectrum did not move more than 10 μm from the center of the field of view of the spectrometer as the analysis energy was swept from 20 to 2500 eV. For 100 eV pass energies, the field of view of the electron spectrometer is greater than 200 μm diameter. (iv) Finally, corrections were made online for the counting losses associated with the dead times of the multianode microchannel plate detector and its preamplifiers. The procedure for this correction is described in detail elsewhere[24] and is most important at low kinetic energies (below about 100 eV), where the count rate is the highest.

The alignment of the gun and spectrometer and the positioning of the sample surface at the intersection of their respective axes were found to be a very important aspect of this work. As the instrument is basically an energy analyzing, UHV, scanning electron microscope it is provided with facilities for this alignment. It is unusual for conventional electron spectrometers to be equipped with such facilities.

B. Sample preparation and data acquisition

A UHV compatible sample holder supplied by Geller Microanalytical Laboratory (Geller Microanalytical Laboratory, Peabody, Mass.) containing 32 elemental samples comprising 29 metals (Be, C, Mg, Al, Ti, V, Cr, Mn, Fe, Co, Ni, Cu, Y, Zr, Nb, Mo, Rh, Pd, Ag, In, Sn, Ta, W, Re, Ir, Pt, Au, Pb, and Th), 2 semiconductors (Si,Ge) and a bulk insulator (B) was employed in this investigation. Each sample was approximately 3 mm in diameter and was mechanically polished with fine Al_2O_3 powder prior to insertion in the holder. The center location of the holder was occupied by a small aperture, which formed a Faraday cup allowing measurement of the electron beam current.

After insertion in the instrument and following baking of the system for approximately 24 h at 140 °C, the samples were cleaned by repeated periods of ion bombardment with 3 keV Xe^+. A number of samples proved difficult to clean and retained small residual amounts of O and C after several cleaning periods. Spectra from all 32 elements were collected in a single session in order to minimize any possible effects due to long-term changes in the properties of the instrument. All spectra were collected with a beam energy of 20 keV, a beam current of approximately 8.4 nA and an analyzer pass energy of 100 eV. The beam current was monitored at regular intervals during the collection of spectra to ensure that it remained constant. The angle of incidence and the take-off angle into the spectrometer (both measured from the surface normal) were both 32° for two sets of data. Another set of data was acquired with an angle of incidence of 45° but this change did not make any significant difference to the values of A and m that were subsequently measured.

All of the spectra were corrected for the instrument function constructed from the C spectrum collected in each data set. The background in this spectrum was modeled by carrying out a nonlinear least-squares fit of Eq. (1) using the algorithms described by Trebbia[28] between 600 and 850 eV. The spectrometer characterization experiments had revealed that the internal scattering effects were smaller than 1% of the true background within this energy range provided that the pass energy was 100 eV or greater. Further, electron optical modeling had revealed that the spectrometer transmission function was constant up to 1000 eV. The instrument function could therefore be estimated by taking the ratio of the measured spectrum and the modeled section extrapolated over the whole energy range of the measurements. The three instrument functions (one for each set of measurements) were averaged together and this is shown in Fig. 2 for a 100 eV pass energy. The differences between the three instrument functions are small and are most likely to be due to changes in the secondary electron yields of the metallic surfaces of the spectrometer subsequent to each bombardment of the C sample with Xe^+ ions. Minor amounts of sputtered C may have reached the surfaces of the spectrometer and modified the secondary electron yields. Additionally, small day to day changes in the potentials on the spectrometer components (nominally constant to ± 0.25 V) and small errors in the positioning of the sample can cause tiny variations in the instrument function.

The corrected spectra were then analyzed using Trebbia's nonlinear least-squares fitting method. With the exception of the Be-C and Ti-Ge groups of elements, the values of A and m were estimated using the 650–850 eV section of the spectra. Again, this was selected both

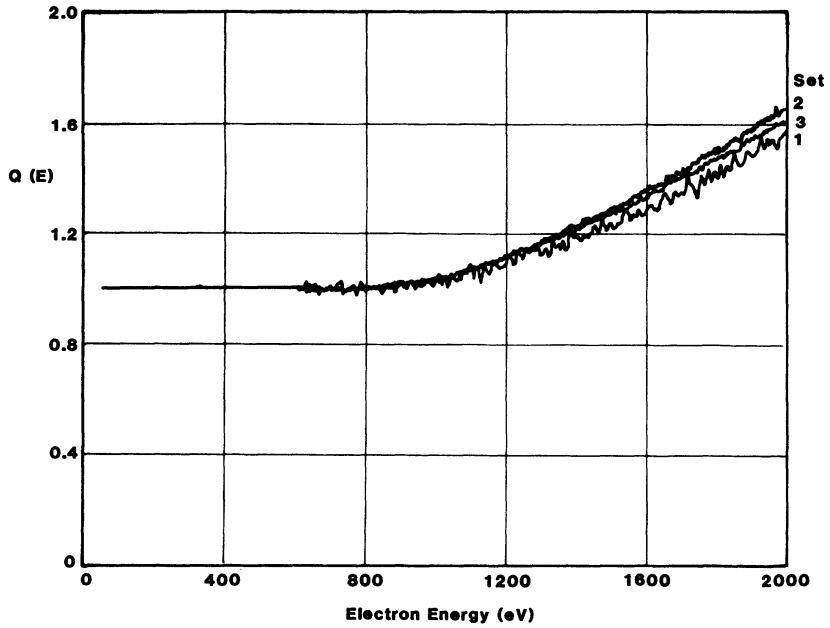

FIG. 2. The instrument function, which includes both transmission function and the internal scattering effects. It was constructed from the average of the carbon spectra in each of three sets as described in the text.

because it is free of any Auger features for most elements in these groups and because this is the range shown by the spectrometer characterization to have the lowest internal scattering effects and, as mentioned previously, the transmission is considered to be constant in this energy range. In some instances there are Auger features above 850 eV and, because of multiple inelastic scattering, these internal sources will make a contribution to the background at lower energies. The values of A and m for the Be-C group were calculated from the spectral energy range 800–2000 eV. This range was selected because there was evidence of tiny amounts of contamination (possibly traces of Fe sputtered from the sample holder during cleaning) in the B spectra in the energy range 600–800 eV. In the Ti-Ge group there are Auger features in the 650–850 eV range for many of the elements, therefore A and m were calculated from the section of the spectrum extending from just above the highest-energy Auger peak to 2000 eV. These procedures for evaluating A and m in the Be-C and Ti-Ge groups are dependent upon the instrument response function and are therefore subject to a small systematic error.

IV. RESULTS

The spectra obtained after correction for the instrument function and normalization to a beam current of 8.4 nA are shown superposed and plotted in the $\log_{10}[N(E)]$ versus $\log_{10}(E)$ form in Figs. 3–6. For the sake of clarity the spectra have been displaced in the vertical direction by multiplying them by successive powers of 1.5. In the case of the Th spectrum an additional factor of 1.5 was required to separate it from the Pb spectrum. The linear nature of the secondary electron cascade when plotted in

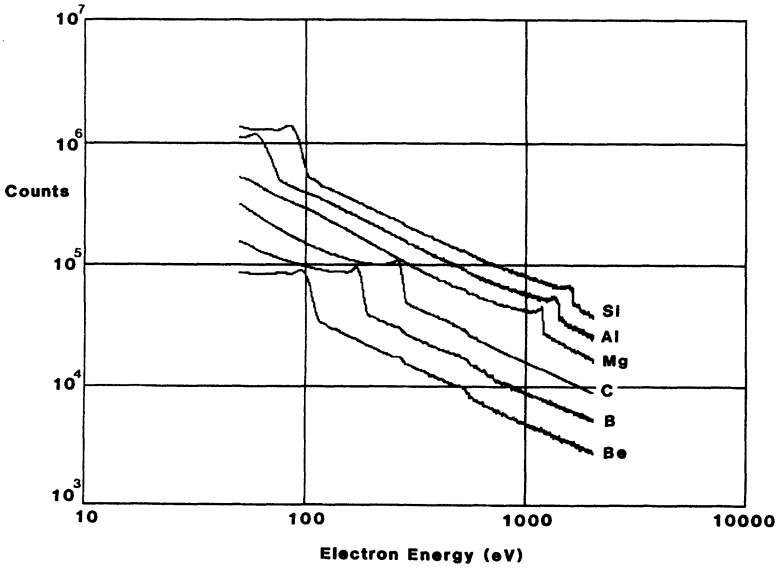

FIG. 3. Spectra of the Be-Si group of elements recorded with a beam energy of 20 keV and a spectrometer pass energy of 100 eV using 8.4 nA of beam current with a scanned area of side 80 μm. The spectra are the sum of 5 scans with a dwell time of 100 ms per energy channel and energy steps of 0.25 eV. The data are presented as plots of the logarithm of the measured count versus the logarithm of the kinetic energy in order to compress the display and to reveal the linear sections expected from a power-law energy dependence of the cascade. The spectra have been multiplied successively by 1.5 in order to displace them vertically in this presentation.

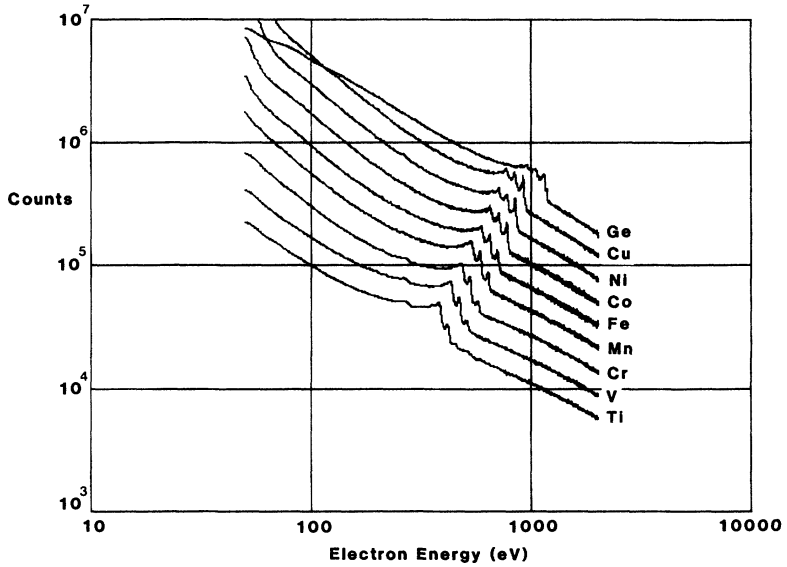

FIG. 4. Spectra of the Ti-Ge group of elements. Conditions as in Fig. 3.

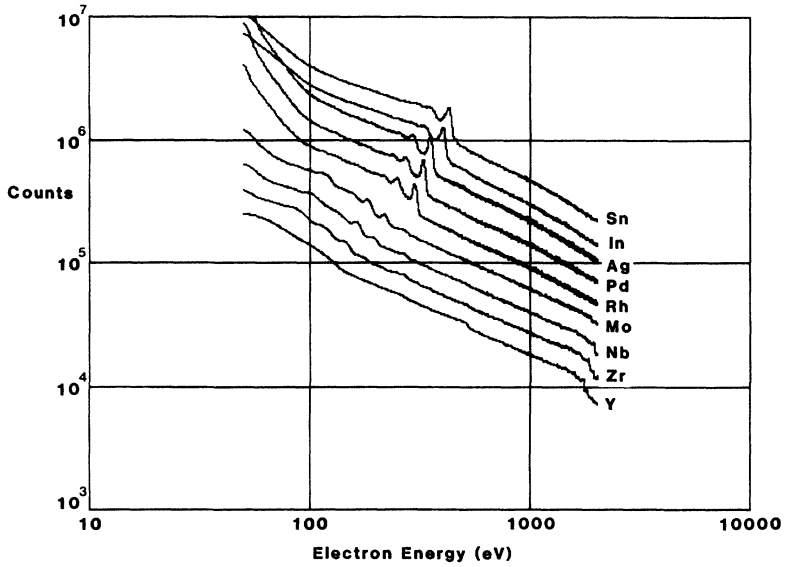

FIG. 5. Spectra of the Y-Sn group of elements. Conditions as in Fig. 3.

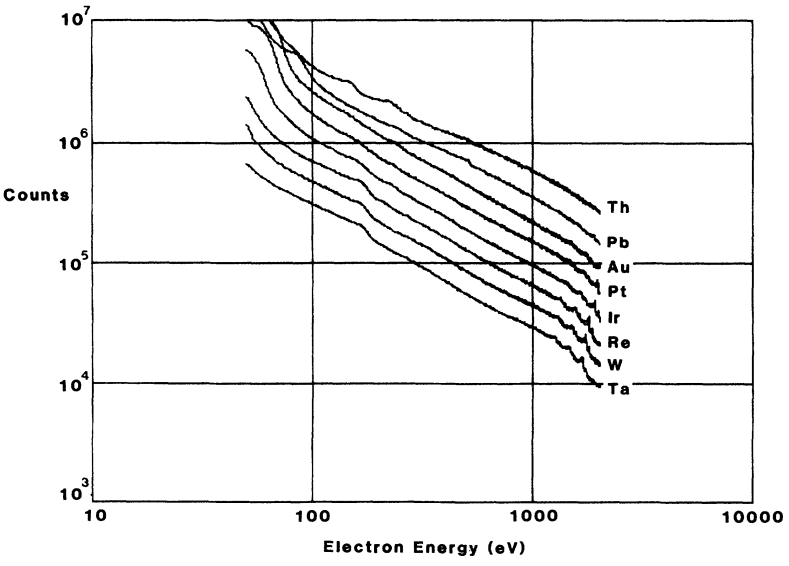

FIG. 6. Spectra of the Ta-Th group of elements. Conditions as in Fig. 3. The spectrum for Th is included here for convenience. It should be noted that Th belongs to the next row of elements in the Periodic Table. The Th spectrum has been multiplied by *additional* factor of 1.5 in order to separate it from the Pb spectrum.

this form is clearly evident. Superposition in the direct $N(E)$ versus E mode (not shown) revealed very clearly that all spectra have very similar heights at energies near to 2000 eV. This is in agreement with results published by Bishop,[29] who was examining spectra to find a means for correcting measured data for the effects on the Auger yield of the surface roughness and the subsurface atomic number. The values of A and m in Table I are the means derived from the three data sets and are plotted in Figs. 7 and 8 as functions of the atomic number.

The random errors in the values of m are estimated to be of the order of ± 0.03. There are also potential systematic errors in the estimation of m because it has not been possible to establish an absolute instrument function for the spectrometer or find an absolute spectrum measured at 20 keV, which can be used as a standard. Any error in the instrument function, which can be approximated as a power of the kinetic energy will give an additive contribution to the value of m and a scaling factor in the estimation of A. This is put at a maximum of about ± 0.15 in m. This problem shows up, for example, in a comparison of the values for m appropriate to carbon reported in Table I and in the spectrometer characterization paper (Ref. 26). These are 0.82 and 0.52, respectively. The discrepancy arises because of the different methods used to derive an instrument function from the given data. In Ref. 27, the B and Be spectra were fitted with a power law over the range 800–1200 eV and then the raw spectra were ratioed with the fitted power-law function. The two estimates of the instrument function were then averaged together and used to correct the spectra of the other elements over the whole range of 200–2500 eV. This is subject to a greater systematic error than the approach described in the present work because of the effects of extrapolating over such a wide region. Therefore, the data reported here are regarded as more accurate than the values of m cited in the instrument characterization paper. It should be stressed both that the power-law fits the region of the background, which is free from Auger features with residuals of less than $\pm 1\%$ for all the elements studied and that the pat-

TABLE I. The values of A and m for the different elements. A is in units of counts $nA^{-1}s^{-1}$.

Element	Atomic number	10^6 A	m
	800–2000 eV		
Be	4	0.80	0.71
B	5	1.1	0.73
C	6	2.4	0.82
	600–850 eV		
Mg	12	0.56	0.53
Al	13	0.94	0.62
Si	14	1.2	0.67
	Peak–2000 eV		
Ti	22	3.4	0.81
V	23	4.0	0.83
Cr	24	5.5	0.87
Mn	25	9.2	0.94
Fe	26	9.6	0.94
Co	27	16	1.02
Ni	28	20	1.02
Cu	29	36	1.10
Ge	32	49	1.15
	600–850 eV		
Y	39	2.9	0.73
Zr	40	3.2	0.74
Nb	41	2.9	0.72
Mo	42	2.9	0.72
Rh	45	3.7	0.75
Pd	46	3.0	0.76
Ag	47	5.8	0.80
In	49	6.9	0.86
Sn	50	5.4	0.81
	600–850 eV		
Ta	73	14	0.88
W	74	16	0.90
Re	75	21	0.95
Ir	77	23	0.96
Pt	78	23	0.95
Au	79	26	0.97
Pb	82	16	0.88
Th	90	6.1	0.80

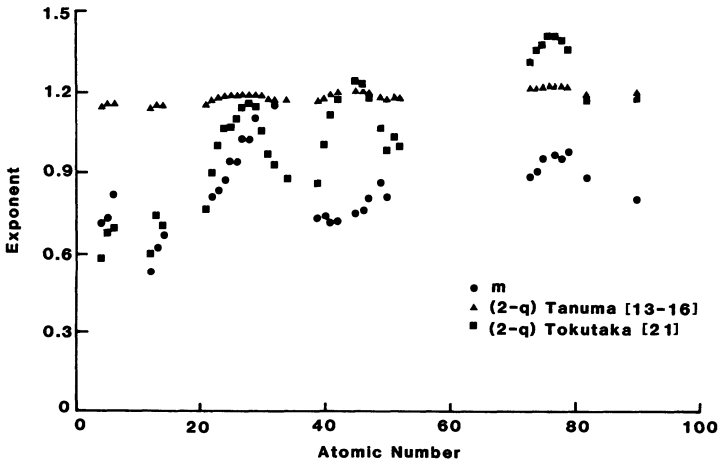

FIG. 7. The variation of the exponent m with atomic number Z. ● are the measured values of m. ▲ are the values of $(2-q)$ for the Tanuma, Powell, and Penn exponent q after correction for elastic scattering. ■ are the values of $(2-q)$ for the exponent q of the attenuation length of Tokutaka, Nishimori, and Hayashi.

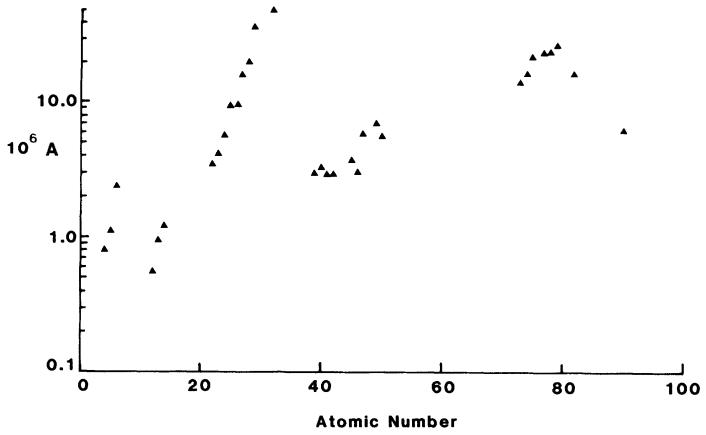

FIG. 8. The measured variation of the preexponential A as a function of atomic number.

terns in A and m with varying atomic number are not changed by any such systematic errors.

The first observations that can be drawn from Fig. 7 and Table I are that the m values vary between 0.53 and 1.15 and that there is a systematic behavior with Z, which shows the same pattern as the variations in the number of valence electrons per atom displayed in the Periodic Table of the elements. The variations across the first and second transition series are particularly clear. Some caution should be exercised in interpreting the values of m and A in the elements Mg-Si because the inelastic tail below the KLL Auger peaks extends over a wide energy range and may have led to underestimates of both parameters. Also, the elements Ta to Pb include very small Auger peaks in the energy range used to estimate m and A. This may result in a noticeable error in the estimation of the two background parameters. Nevertheless it can be concluded that the Seah and Dench and the Szajman equations given above cannot be extended to describe the behavior of m in spite of the fact that both approaches give a reasonable fit to the energy dependence of the attenuation lengths of the elements. On the other hand the observed values of m are within the range of 0.5–1.5 predicted by Matthew and coworkers.[12,31] The attenuation lengths calculated from the imfp expression TPP-2 and given from experimental data due to Tokutaka, Nishimori, and Hayashi (Fig. 1) do show variations with Z and these are shown in Fig. 7 as $(2-q)$ as predicted using Eqs. (4) and (7).

Since it is the secondary-electron cascade that is being measured in these experiments, it is to be expected that there may be a relationship between these results and estimates of the atomic number dependence of the secondary electron yield δ. The quantity δ is normally defined to be the number of electrons emitted into the vacuum with energies up to 50 eV for each incident electron. Nevertheless, one might expect that an increase in the area under the secondary-electron cascade will scale with Z in the same way as does δ. Measurements of $\delta(Z)$ have been reported by Makarov and Petrov.[30] Unfortunately, their results are for primary beam energies of 2 keV and extension to 20 keV as used in this work is not simple. Nevertheless, they do observe a periodic behavior of δ with increasing Z.

The measured data are best described by values of $(2-q)$ deduced from the expressions fitted to experimental data for the energy dependence of the attenuation length due to Tokutaka, Nishimori, and Hayashi. Further, they are bounded by $(2-q)$ and $(1-q)$—the latter being the term predicted by Matthew and co-workers for a theory describing fast secondary-electron generation via a Mott cross section and a straight-line approximation for escape of the electrons to the surface after their generation. The straight-line approximation is expected to provide a lower limit to the possible values of m. The measured values of m are closer to $(2-q)$ than to $(1-q)$ suggesting, as expected, that the effects of elastic scattering are not negligible in the energy range used here. The agreement between m and $(2-q)$ is quite good for rows 2, 3, and 4 of the Periodic Table but is poorer for rows 5, 6, and 7. Although elastic scattering is stronger for the higher numbered rows, it should be noted that the values of m have remained very roughly constant, while the values of $(2-q)$ are broadly rising.

The values of $(2-q)$ deduced from the TPP-2 equations have a smaller variation in the exponent than does m and show no sign of the sharply rising behavior with increasing Z as seen in row 4.

The errors in the estimation of A are inevitably larger than those in m because an extrapolation to 1 eV is involved. Figure 8 shows the variation of A with Z where the pattern following the rows of the Periodic Table is evident nevertheless.

It can be seen from the data in Table I that the parameters A and m are strongly correlated. The relationship between them is shown in Fig. 9. The straight line in the figure is the least squares linear regression onto the data—the correlation coefficient between $\log_{10}(A)$ and m being 0.94. Given the observation that the spectra pass through about the same magnitude of $N(E)$ near 2000 eV, it is simple to show that a plot of $\log_{10}(A)$ versus m should have a slope of $\log_{10}(2000)$—about 3.3 The linear regression shown in Fig. 9 has a slope of about 3.5. Thus the spectra shown in Figs. 3–6 are consistent with the relationship between A and m shown in Fig. 9. The physical mechanisms underlying the two parameters must be related through at least one common property of the sample. Such correlations have been sought by exam-

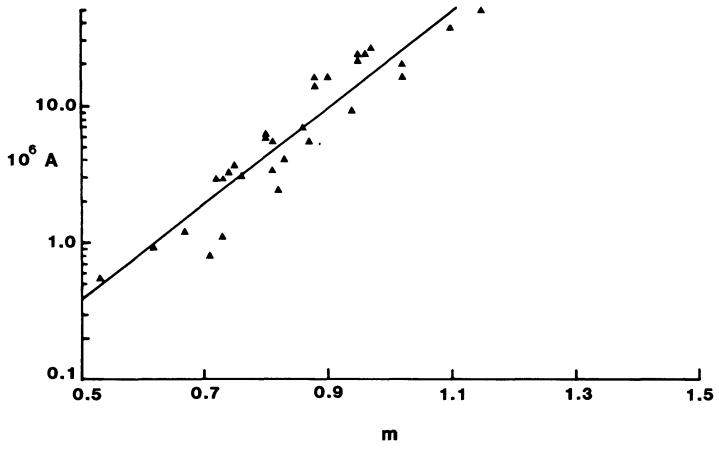

FIG. 9. The relationship between ln(A) and m. The straight line is a linear regression plot on the data. The correlation coefficient between ln(A) and m is 0.94.

ining the atomic number dependence of the valence-band electron density and other related quantities. The strongest correlations are observed between the measured values of A and m and the free electron energy E_p, which is given by

$$E_p = 28.8\sqrt{\rho N_v / M} \text{ eV} \tag{9}$$

for a material with density ρ gm cm^{-3}, N_v valence electrons per atom and atomic weight M. Of course, this is not an expression for the true plasmon energy in a sample—it includes, for example, all the d and s electrons in the first transition series metals. However, it is commonly used to describe an effective free electron energy in theoretical accounts of the physics of the inelastic mean free path (see, for example, Tanuma, Powell, and Penn[13–16] and Sjazman *et al.*[17]). The relationships between E_p and the measured values of A and m are shown in Figs. 10 and 11. It is not surprising that E_p is significant in this way because plasmon excitation is the most probable event caused by electrons on their way to the surface from their point of origin. The correlation of A with E_p^2 is interpretable from Eq. (9) as simply as linear dependence of A upon the density of mobile electrons N_v. Although, to a first approximation, the m values appear to be a roughly linear function of E_p and the A values roughly a linear function of E_p^2, it is clear that the individual periods of the elements are described by slightly different functions.

V. CONCLUSIONS

In spite of the difficulties associated with high-accuracy spectrometer characterization, it is clear that the power law of Eq. (1) is a good description of the shape of the secondary-electron cascade for the 32 elements measured here. Secondly, the values of the exponent m do fall within the extrema of 0.5 and 1.5 predicted by Matthew *et al.* Further, it is clear that there is a pattern in the coefficients A and m as a function of atomic number, which is related to the rows in the Periodic Table and, therefore, to the number of valence electrons per atom. Existing approaches to a description of the energy dependence of the attenuation length in the elements give quite a good account of the experimental data as reviewed by Tanuma, Powell, and Penn and are expected to bear some relationship to the power-law describing the cascade. However, the slope of this energy dependence in

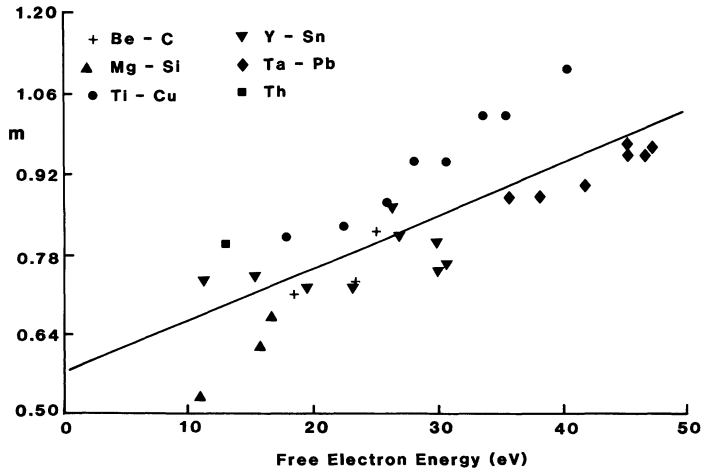

FIG. 10. The relationship between the measured values of m and the free electron energy. Each period has been assigned a different symbol and the straight line has been obtained by linear regression on the complete data set.

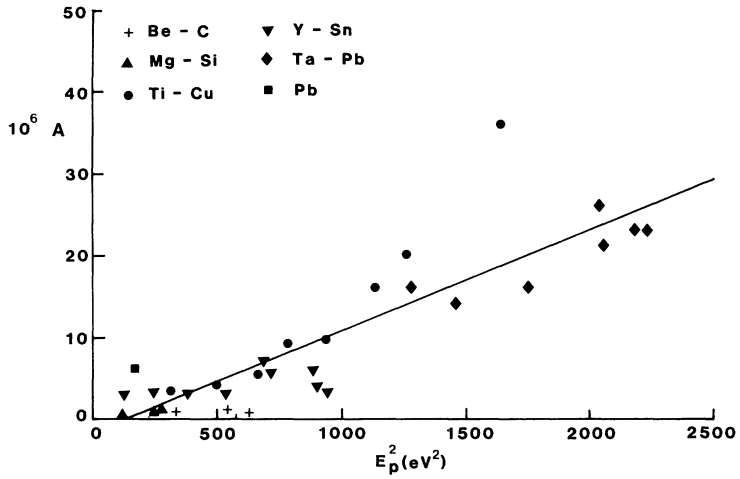

FIG. 11. The relationship between the measured values of A and the square of the free electron energy (and thus the valence electron density). The line has been calculated by linear regression on the complete data set.

the range 400–2000 eV appears to vary considerably between the purely theoretical approaches to the imfp as well as between the experimental fits to measured attenuation lengths. The best agreement between the measured values of m and the exponent q of the power-law describing the energy dependence of the attenuation length is with the empirical expressions of Tokutaka *et al.* and the Sickafus theory leading to the expectation that m and $(2-q)$ are, at least approximately, the same parameter.

Of the two expressions showing energy dependence of the imfp on the one hand and the attenuation length on the other, perhaps it is not too surprising that the Tokutaka, Nishimori, and Hayashi attenuation lengths show a better correlation with m. Seah's modification of the Tanuma, Powell, and Penn TPP-2 expression for the imfp takes no account of multiple scattering or the attenuation of the primary beam. The equations of Tokutaka, Nishimori, and Hayashi for the attenuation length are based upon experimental data and so automatically include all the effects of scattering in the solid. Thus they are more likely to be comparable with an experimental measurement of the related quantity, m. However, they remain an unsatisfactory description of the processes involved in the sense that they are based upon a pragmatic interpretation of experimental measurements rather than a theoretical examination of the physics of the scattering problem.

The examination of the relationships between the parameters A and m and the free electron plasmon energy E_p suggests that Eq. (1) can be recast in the form

$$B(E) \approx \alpha N_v E^{-(\beta+\gamma E_p)}, \tag{10}$$

where α, β, and γ are material independent parameters. The beam energy has been subsumed into the parameter α and is likely to appear in the parameter γ. More theoretical work is needed to include the energy dependence of the imfp, elastic scattering, and the effects of the finite binding energies of electrons contributing to the secondary cascade in the transport process to the surface before this result can be interpreted in more detail. A start has been made in this direction by Matthew *et al.*[31] using Monte Carlo methods and simple analytic models to investigate the shape of the secondary-electron background.

ACKNOWLEDGMENTS

The authors are pleased to be able to thank the Science and Engineering Research Council for grants supporting this work. They would also like to thank I. R. Barkshire, P. G. Kenny, M. M. El Gomati, and J. A. D. Matthew for their help with the instrument and many useful discussions.

*Permanent address: Department of Physics, University of Newcastle, Callaghan 2308, New South Wales, Australia.

[1]E. N. Sickafus, Phys. Rev. B **16**, 1436 (1977).
[2]E. N. Sickafus, Phys. Rev. B **16**, 1448 (1977).
[3]E. N. Sickafus and C. Kukla, Phys. Rev. B **19**, 4056 (1979).
[4]P. A. Wolff, Phys. Rev. B **95**, 56 (1954).
[5]H. Stolz, Ann. Phys. (Leipzig) **3**, 197 (1959).
[6]G. F. Amelio, J. Vac. Sci. Technol. **7**, 593 (1970).
[7]A. J. Bennett and L. M. Roth, Phys. Rev. B **5**, 4309 (1972).
[8]M. P. Seah, Surf. Sci. **17**, 132 (1969).
[9]Y. E. Strausser, D. Franklin, and P. Courtney, Thin Solid Films **84**, 145 (1981).
[10]D. C. Peacock, D. C. Peacock, and R. H. Roberts, Vacuum TAIP **34**, 497 (1984).
[11]D. C. Peacock and J. P. Duraud, Surf. Interface Anal. **8**, 1 (1986).
[12]J. A. D. Matthew, M. Prutton, M. M. El Gomati, and D. C. Peacock, Surf. Interface Anal. **11**, 173 (1988).
[13]S. Tanuma, C. J. Powell, and D. R. Penn, Surf. Interface Anal. **20**, 77 (1993).
[14]S. Tanuma, C. J. Powell, and D. R. Penn, Surf. Interface Anal. **11**, 577 (1988).

[15]S. Tanuma, C. J. Powell, and D. R. Penn, Surf. Interface Anal. **17**, 911 (1991).
[16]S. Tanuma, C. J. Powell, and D. R. Penn, Surf. Interface Anal. **17**, 927 (1991).
[17]J. Szajman, J. Liesegang, J. G. Jenkin, and R. C. G. Leckey, J. Electron Spectrosc. Relat. Phenom. **23**, 97 (1981).
[18]D. Briggs and M. P. Seah, *Practical Surface Analysis by Auger and X-ray Photoelectron Spectroscopy* (Wiley, Chichester, 1992).
[19]M. P. Seah and W. A. Dench, Surf. Interface Anal. **1**, 2 (1979).
[20]C. D. Wagner, L. E. Davis, and W. M. Riggs, Surf. Interface Anal. **2**, 53 (1980).
[21]H. Tokutaka, K. Nishimori, and H. Hayashi, Surf. Sci. **149**, 349 (1985).
[22]A. Jablonski, Surf. Sci. **151**, 166 (1985).
[23]M. P. Seah, in *Quantitative Microbeam Analysis* (Institute of Physics, Bristol, 1993).
[24]M. Prutton, C. G. H. Walker, J. C. Greenwood, P. G. Kenny, J. C. Dee, I. R. Barkshire, and R. H. Roberts, Surf. Interface Anal. **17**, 71 (1991).
[25]M. P. Seah and G. C. Smith, Surf. Interface Anal. **15**, 751 (1990).
[26]M. P. Seah, Surf. Interface Anal. **20**, 865 (1993).
[27]J. C. Greenwood, M. Prutton, R. H. Roberts, and Zhixiong Liu, Surf. Interface Anal. **20**, 891 (1993).
[28]P. Trebbia, Ultramicroscopy **24**, 399 (1988).
[29]H. E. Bishop, *Electron Beam Interactions with Solids for Microscopy, Microanalysis and Micro-lithography* (SEM Inc., AMF O'Hare, IL, 1984), p. 259.
[30]V. V. Makarov and N. N. Petrov, Fiz. Tverd. Tela (Leningrad) **23**, 1767 (1981) [Sov. Phys. Solid State **23**, 1028 (1981)].
[31]J. A. D. Matthew, W. C. C. Ross, and M. M. El Gomati, Inst. Phys. Conf. Ser. **130**, 383 (1993).